Stroke A Journal of Cerebral Circulation
Issue: Volume 26(6), June 1995, pp 1086-1091

Publication Type: [Original Contribution]
ISSN: 0039-24990039-2499
Accession: 7762027
Keywords: Animals, Blood Pressure, Brain Ischemia, Brain Ischemia, Cerebral Cortex, Cerebral Cortex, Cerebral Cortex, Craniotomy, Disease Models, Animal, Electroencephalography, Laser-Doppler Flowmetry, Male, Perfusion, Rats, Rats, Sprague-Dawley, Regression Analysis, Subarachnoid Hemorrhage, Subarachnoid Hemorrhage, Time Factors

[Original Contribution]

Cortical Blood Flow and Cerebral Perfusion Pressure in a New Noncraniotomy Model of Subarachnoid Hemorrhage in the Rat

Bederson, Joshua B. MD; Germano, Isabelle M. MD; Guarino, Lorraine BS

Author Information

Received September 19, 1994; final revision received December 6, 1994; accepted February 27, 1995.
From the Department of Neurosurgery, The Mount Sinai School of Medicine, New York, NY.
Correspondence to Joshua B. Bederson, MD, Department of Neurosurgery, Box 1136, The Mount Sinai School of Medicine, 1 Gustave L. Levy Pl, New York, NY 10029.

Abstract

Background and Purpose: Acute cerebral ischemia after subarachnoid hemorrhage (SAH) is a major cause of morbidity whose precise etiology is unclear. The purpose of this study was to examine the relationships between cerebral perfusion pressure (CPP) and cortical blood flow during SAH using a new experimental model in the rat.

Methods: CPP (mean arterial pressure minus intracranial pressure), cortical laser-Doppler flowmetry (LDF), and electroencephalogram were continuously recorded during and after SAH in 16 ventilated rats. SAH was produced by advancing an intraluminal suture from the external carotid artery through the internal carotid artery to perforate the vessel near its intracranial bifurcation.

Results: Eight rats (50%) died within 24 hours of SAH. In all rats, blood was widely distributed throughout the basal, convexity, and interhemispheric subarachnoid spaces and throughout the ventricular system. CPP decreased after SAH at an initial rate of 1.1 plus minus 0.2 mm Hg/s, reaching its nadir 59 plus minus 9 seconds after the onset of SAH. During the same period, LDF fell at a rate of 1.4 plus minus 0.3%/s (P equals NS vs CPP). After reaching its nadir, CPP rose at a rate of 0.4 plus minus 0 .01 mm Hg/s, but LDF continued to fall at 0.2 plus minus 0 .03%/s (P less than .05 vs CPP) reaching a nadir of 21.7 plus minus 2.5% significantly later than CPP (189.5 plus minus 39 s after SAH, P less than .05). No correlation was found between peak changes in CPP and LDF. Electroencephalogram activity followed the changes in LDF, reaching nadir values 289 plus minus 55 seconds after SAH.

Conclusions: These findings demonstrate that although reduced CPP causes the initial decrease in cortical blood flow after SAH, secondary reductions occurring after CPP has reached its nadir are caused by other factors such as acute vasoconstriction. This noncraniotomy model of SAH in the rat has several advantages over existing models.

(Stroke. 1995;26:1086-1092.)

Key Words: animal models, cerebral blood flow, hemodynamics, subarachnoid hemorrhage, rats

Subarachnoid hemorrhage (SAH) causes brain injury both acutely and as the result of delayed vasospasm. Despite progress in understanding and treating delayed ischemia, acute brain damage is the primary cause of mortality after SAH, [1] yet its etiology remains unclear. Acute cerebral ischemia is an important contributor to brain damage in this setting, as demonstrated in patients who die shortly after SAH, in whose brains extensive ischemic damage is seen. [2] Acute ischemia from SAH has been attributed to decreased cerebral perfusion pressure (CPP), [3] and this is supported by data from repeat hemorrhages in humans with intracranial pressure (ICP) monitors. [4,5] However, brain compliance is reduced by the initial bleed and may lead to greater rises in ICP during the second bleed. Experimental studies of first-time hemorrhages demonstrate that CPP does not drop to the point of perfusion arrest. [6-8] Physiological data suggest that decreased CPP cannot fully account for acute ischemic brain damage after SAH. [5-7,9,10] However, previous studies have used time-averaged or intermittent measurements of cerebral blood flow (CBF) that may not demonstrate acute changes after SAH. Such changes could be evaluated by use of an experimental model with continuous recordings of CBF.

Currently available animal models of SAH [6,8-17] are limited by the need for craniotomy and arachnoidal dissection or surgical placement of an infusion catheter, by the use of dorsal cisterns rather than the basal

subarachnoid space, and by catheter-induced dampening of arterial pulsations, small elevations of ICP, or limited distribution of blood.

In this study we investigated a new rat model of SAH that avoids many problems of currently available models and allows continuous undisturbed measurements of cortical blood flow and CPP during the hemorrhage. Based on preliminary results, [18] our primary hypothesis was that acute SAH-induced reductions in CBF are, at least in part, independent of reductions in CPP.

Materials and Methods

Surgical Preparation

All procedures were approved by our accredited animal care committee. Male Sprague-Dawley rats (n equals 22) weighing 250 to 300 g were housed under diurnal lighting conditions and given free access to food and water before and after the experiment. The rats were anesthetized with chloral hydrate (350 mg/kg IP) and intubated transorally with a polyethylene catheter (OD 2.5 mm); anesthesia was maintained with inspired halothane (1% to 2% in O_2-supplemented room air). The right femoral artery was cannulated for monitoring blood gases, and ventilation was adjusted to maintain arterial blood gases in the normal range (PCO_2, 37 plus minus 1 mm Hg; PO_2, 140 plus minus 3 mm Hg; pH 7.37 plus minus 0 .01 [mean plus minus SEM]). Body temperature was monitored with a rectal probe and maintained at 37 degrees C with a homeothermic blanket (Harvard Apparatus).

Rats were placed in a stereotaxic frame (Stoelting) modified to allow longitudinal rotation and permit manipulations with the rat prone or supine. Four 1-mm-diameter burr holes were placed 4 mm lateral, 2 mm rostral, and 2 mm caudal to bregma. Epidural electroencephalogram (EEG) electrodes were hooked under the edge of each burr hole and secured to the stereotaxic frame. Nasion reference and femoral ground electrodes were connected to a custom-built amplifier-computer (see below) to achieve a bilateral hemispheric bipolar EEG montage.

For measurement of cortical blood flow, a 3-mm burr hole was made 5 mm to the left of midline at the coronal suture, and a laser-Doppler flowmetry (LDF) probe (0.8 mm diameter, model P-433, Vasamedics Inc) was advanced under stereotaxic control to the cortical epidural surface away from large pial vessels. The side contralateral to the site of SAH was chosen to ensure that observed changes were attributable to SAH rather than to transient occlusion. A modification of the technique of Barth et al [19] was used to monitor ICP. A burr hole was made in the midline occipital bone to accept a stainless steel screw. A 25-gauge butterfly cannula primed with saline and attached to a pressure transducer centered at the ear bars was advanced through the atlanto-occipital membrane into the cisterna magna until a good ICP waveform was obtained. The cannula was secured to the screw with methylmethacrylate cement. The rat was then rotated into the supine position with all recording devices in place and kept there for the remainder of the experiment.

Induction of SAH

The cerebral ischemia model of Zea-Longa et al [20] was modified to produce SAH. In brief, the right carotid artery was identified along with all its extracranial branches, and the external carotid artery was dissected, transected distally, and reflected inferiorly. A 3-0 monofilament suture with one end sharpened was advanced centripetally into the external carotid artery past the common carotid bifurcation and into the internal carotid artery (ICA). The suture was advanced distally into the intracranial ICA until resistance was felt (at 18 to 20 mm) and then was pushed 3 mm further, penetrating the ICA near its intracranial bifurcation (n equals 18). Preliminary studies in 4 rats showed that the suture penetrated the ICA, middle cerebral artery, or anterior cerebral artery within 1 mm of the intracranial bifurcation. The suture was then withdrawn into the external carotid artery, reperfusing the ICA and producing SAH Figure 1. [18] The duration of endovascular occlusion was 30 seconds to 4 minutes. Four sham-operated control rats underwent an identical procedure except that the suture was not advanced beyond the point of resistance; reperfusion occurred after 4 minutes of occlusion. After each experiment, the ICP catheter was crimped and cut at its attachment to the occipital screw, which was left in situ. Rats were returned to single, warmed cages while still intubated for airway protection. Self-extubation occurred as the rats recovered from anesthesia, usually within 30 minutes. Rats underwent neurological examination after recovery from anesthesia and 24 hours after SAH, as previously described, [21] and were killed after the second examination.

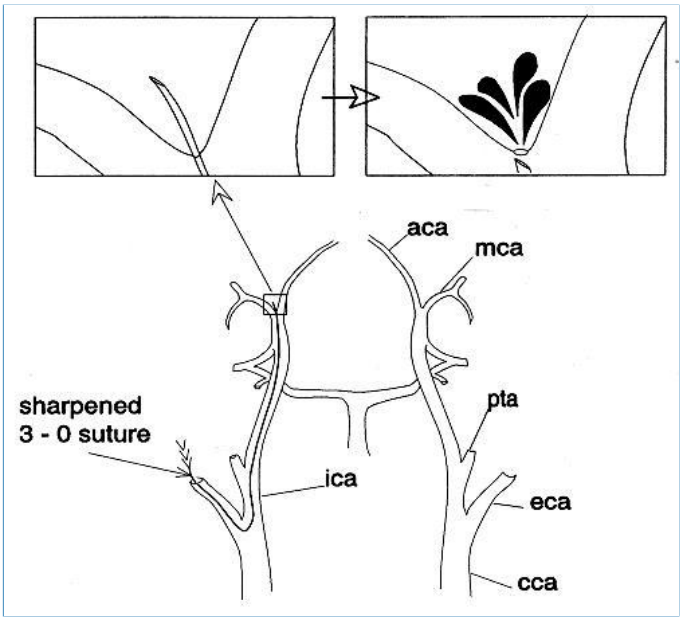

Figure 1. Diagram shows endovascular suture technique for inducing subarachnoid hemorrhage. A 3-0 monofilament suture sharpened at one end is introduced through the external carotid artery (eca) and advanced through the intracranial internal carotid artery (ica), penetrating near the bifurcation. Withdrawal of the suture results in subarachnoid hemorrhage. aca indicates anterior cerebral artery; mca, middle cerebral artery; pta, ptery-gopalatine artery; and cca, common carotid artery.

Data Acquisition and Storage

Blood pressure, LDF, ICP, and EEG waveforms were processed and stroed on a Macintosh Quadra 950 (Apple Computer Inc) by use of customized analog-to-digital signal conversion and processing hardware and software from National Instruments (SCSI, NB-MIO16XL, LABVIEW 3 .0). The system was configured to acquire 16 bipolar signals at sampling rates of 1024 Hz. The EEG signal was processed on-line with a fast Fourier transform at 4-second intervals, and the resulting spectrum was divided into power bands. LDF, ICP, mean arterial pressure (MAP), and the amplitude (mu V sup 2) of the delta power band (1 to 4 Hz) were logged at 0.25 Hz. CPP, defined as MAP minus ICP, was computed for each pair of simultaneously logged data points. LDF data were normalized by comparing each 4-second epoch to the average of all values obtained during a 10-minute baseline before SAH, and are expressed as a percent of baseline. After each experiment, the data were converted to spreadsheet format for graphic analysis (KALEIDEGRAPH, Synergy Software Inc) and statistical analysis (STATVIEW 4 .01, Abacus Concepts Inc).

Statistical Analysis

For comparing serial changes in different animals, the x-axis (time) was set to zero at the onset of SAH, defined as the initial positive deflection in ICP. For determining the statistical significance of changes in CPP, LDF, and EEG, the values in each rat 15 seconds before and 15 seconds after their maximum deflections and at 25 and 50 minutes after SAH were averaged to avoid potential sampling errors due to minor variations in the onset of SAH. The rate of change was expressed as the slope of linear regression derived from CPP or LDF versus time, and averages were compared by use of Student's t test. [22]

Repeated-measures ANOVA was used for serial comparisons, and the Bonferroni correction for post hoc analysis was applied; P less than .05 was considered significant. Minimum LDF and minimum CPP (mCPP) were determined for each rat as described above, and regression analysis was performed on pooled minimum LDF versus minimum CPP data. Data are expressed as mean plus minus SEM.

Histological Examination

Brains were frozen at minus 22 degrees C, and serial coronal sections 10 micro meter thick were cut in a cryostat at minus 20 degrees C and mounted on subbed slides. Sections were stained with Luxol blue (0.1%), counterstained with buffered cresyl violet (2% in 100 mL of phosphate buffered saline, pH 7.4), and exposed to diamino-benzidine. Other sections were hydrated and stained with Wright's solution (1%).

Results

None of the sham-operated control rats showed evidence of subarachnoid blood. Two experimental rats (11%) had large intracerebral hemorrhages and were excluded from the analysis. The remaining experimental rats had extensive SAH. Blood was consistently distributed along the basal, perimesencephalic, and convexity meninges bilaterally, along the interhemispheric fissure and corpus callosum, and, to a lesser extent, within the ventricular system Figure 2.

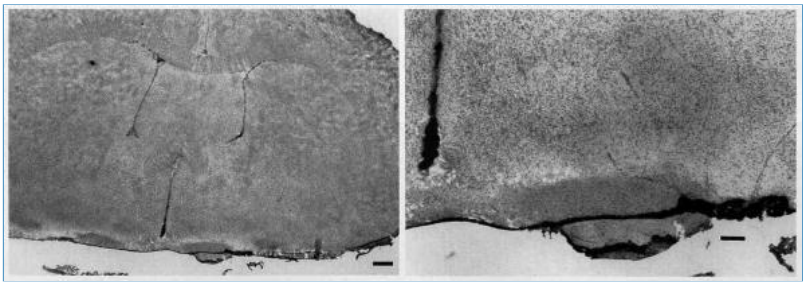

Figure 2. Photomicrographs show coronal sections of rat brain obtained 24 hours after subarachnoid hemorrhage and stained with Luxol blue. Left, Low-power magnification (bar indicates 500 mu m) shows blood distributed throughout the basal and convexity meninges, third and lateral ventricles, and interhemispheric fissure. Note punctate hemorrhage in the basal ganglia. Right, Higher-power magnification (bar indicates 100 mu m) shows blood layered thickly in the subarachnoid space and third ventricle.

There were no significant differences in pH, PCO_2, PO_2, or body temperature before and 30 minutes after SAH Table 1. Rats were initially lethargic after recovering from anesthesia, but no rat had a focal neurological deficit. Eight of 16 (50%) experimental rats died less than 24 hours after SAH, 2 within 2 hours, and 6 within 12 to 24 hours after SAH.

Physiological Data

CPP, LDF, ICP, and EEG tracings from an individual rat during experimental SAH are shown in Figure 3. Pooled data from all 16 rats are shown in Figure 4. CPP, LDF, and EEG activity all decreased rapidly after the onset of SAH. Initially, the changes in CPP and LDF were similar, but approximately 1 minute after SAH, CPP began to rise from its nadir while LDF continued to fall. CPP decreased from 96.3 plus minus 0.5 mm Hg before SAH to 32 .0 plus minus 6.3 mm Hg after SAH, reaching its nadir 59.1 plus minus 9 seconds after the onset of SAH. The average rate of change in CPP, expressed as the slope of CPP versus time from the onset of SAH to mCPP, was minus 1.1 plus minus 0.2 mm Hg/s. During this same period, LDF decreased at an average rate of 1.4 plus minus 0.3%/s to 44 plus minus 4.9% of baseline. This rate of change was not significantly different from that of CPP during the same period. After reaching its nadir, CPP rose toward the baseline at an initial rate of 0.4 plus minus 0 .01 mm Hg/s. During the same period, LDF continued to fall at a rate of 0.2 plus minus 0.3%/s. This was significantly different from both the initial rate of change in LDF (P less than .05) and the rate of change in CPP during the same period (P less than .05). LDF reached a nadir of 21.7 plus minus 2.5% of baseline 189.5 plus minus 39 seconds after SAH, significantly after CPP reached its nadir Figure 4. Linear regression analysis demonstrated no significant relationship between minimum LDF and minimum CPP (y equals 17 minus 0 .01x, r equals .01; P equals NS) Figure 5.

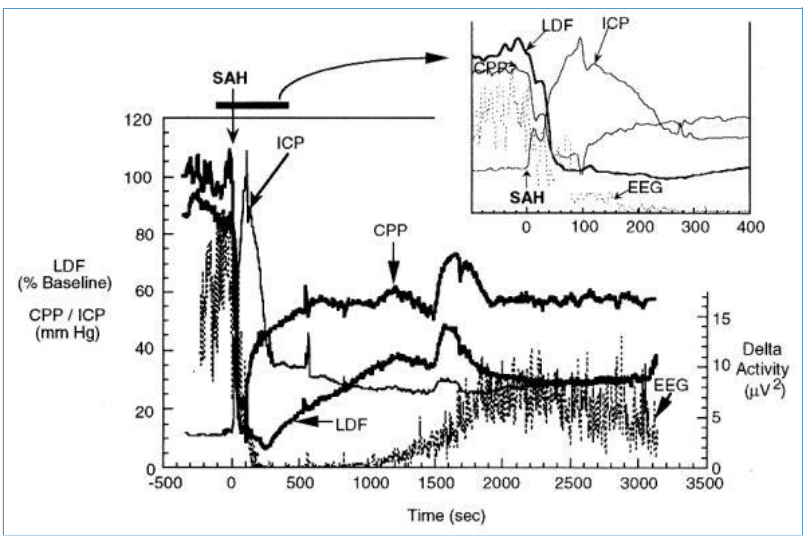

Figure 3. Tracings show continuously recorded laser-Doppler flowmetry (LDF), intracranial pressure (ICP), cerebral perfusion pressure (CPP), and electroencephalogram (EEG) in a rat during subarachnoid hemorrhage (SAH). CPP (in mm Hg) decreased from the middle 80s to a nadir of 10 at 95 seconds after the onset of SAH and then rose toward the baseline, stabilizing near 60. LDF continued to decrease after CPP reached its nadir, falling

to 8% of baseline 245 seconds after the onset of SAH and rising gradually to near 35% of baseline. EEG activity declined after the onset of SAH, reaching its nadir 265 seconds later.

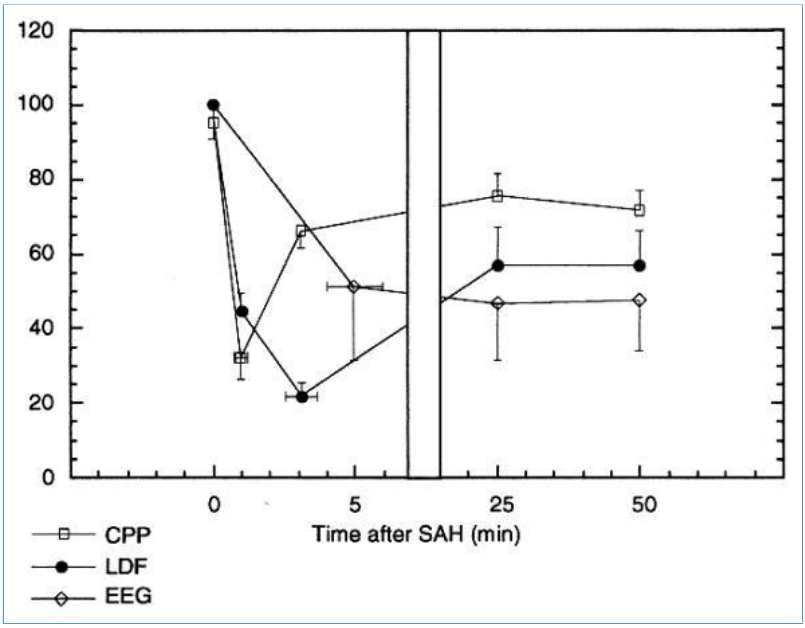

Figure 4. Graph shows average cerebral perfusion pressure (CPP), cortical laser-Doppler flowmetry (LDF), and electroencephalographic (EEG) activity after subarachnoid hemorrhage (SAH) in 16 experimental rats. CPP reached its nadir 59 plus minus 9 seconds after SAH, while LDF fell at a similar rate to 44 plus minus 4.9% of baseline. LDF continued to fall, reaching its nadir 189 plus minus 34 seconds after SAH, while CPP rose to 66 plus minus 6.2 mm Hg. EEG declined to 51 plus minus 24% of baseline over 289 plus minus 55 seconds, and remained unchanged for 50 minutes.

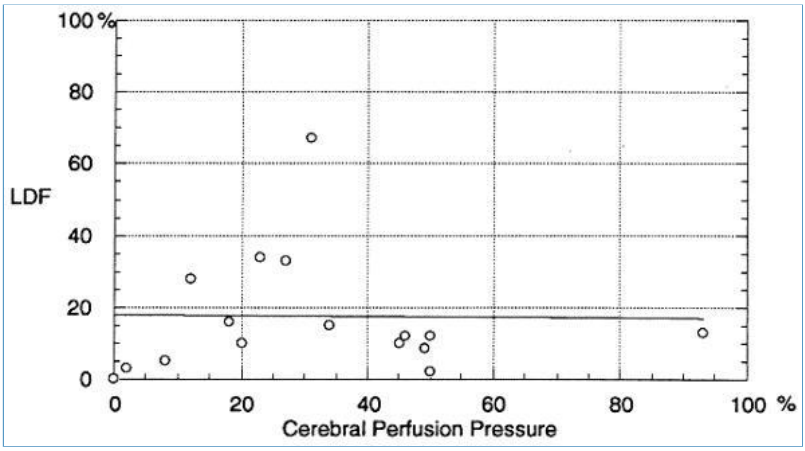

Figure 5. Plot of linear regression analysis indicating no significant relationship between minimum cortical blood flow measured by laser-Doppler flowmetry (LDF) and cerebral perfusion pressure immediately after SAH in 16 rats. Data are normalized to 10-minute baseline.

By 25 and 50 minutes after the onset of SAH, CPP was 75.5 plus minus 6.1 and 71.7 plus minus 5.3 mm Hg and LDF was 56.8 plus minus 10.3% and 51.7 plus minus 9.6% of baseline, respectively. For both measures, these values were significantly greater than the nadir values but less than baseline (P less than .05). EEG delta activity fell to 51.2 plus minus 24% of baseline after SAH (P less than .05), reaching its nadir 289 plus minus 55 seconds after SAH, significantly later than CPP or LDF. By 25 and 50 minutes after SAH, EEG delta activity was unchanged at 46.5 plus minus 15% and 47.8 plus minus 14% of baseline, respectively. Sham-operated rats had no changes in CPP, LDF, or EEG activity contralateral to the endovascular suture.

Discussion

The endovascular suture model of SAH in rats described here reliably produces severe SAH while avoiding some limitations of existing models. Although craniotomy was used to measure LDF and burr holes were used for the EEG in this experiment, the model does not require craniotomy or arachnoidal dissection to produce SAH and thereby eliminates the histological effects such manipulations can have. The model uses focal puncture of the native ICA, allows continuous physiological monitoring during the SAH, results in extensive distribution of blood

throughout the subarachnoid space, reduces cortical blood flow, and produces consistent and significant elevations of ICP.

A potential disadvantage of our model is the brief period of ischemia caused by the intraluminal suture. Endovascular middle cerebral artery occlusion produces infarction unless reperfusion occurs within 30 minutes. [20] In this experiment, less than 4 minutes of transient middle cerebral artery occlusion was required, and as we have accumulated experience in subsequent studies this has been reduced to 30 to 60 seconds. This duration of focal ischemia is significantly shorter than that required to produce infarction. [23] Control rats had no reductions in contralateral LDF or EEG and no evidence of ischemic histological change at 24 hours. Therefore, all changes observed in the experimental rats were due to the hemorrhage. Another disadvantage of the model is the incidence of intracerebral hemorrhage (11% in this series). Finally, 50% of rats died less than 24 hours after SAH. An analysis of the physiological predictors of mortality in this model, an investigation of histological changes 3 and 7 days after SAH, and histopathological studies of the intracranial vessels for evidence of delayed vasospasm are the subjects of a future report.

Measurement of CBF After SAH

Previous studies of CBF after SAH in humans and animals have used time-averaged or discrete point-in-time determinations obtained by a variety of techniques, including radiolabeled microspheres, [13] single photon emission computed tomography, [24-26] xenon computed tomography, [27,28] hydrogen clearance, [29] autoradiography, [30] or positron emission tomography. [31] These studies have shown that average CBF measured shortly after SAH is 50% to 60% of baseline values. In contrast, using LDF as a continuous measure of cortical perfusion, we observed dynamic flow changes after SAH, with transient decreases to 22% of baseline. These brief decreases would be underestimated or missed by time-averaged or single measurements of CBF. In addition, comparison of LDF with CPP during the acute phases of SAH demonstrated temporal and quantitative relationships between these two variables that cannot be observed with other measures of CBF.

LDF has the disadvantage of being an unreliable indicator of absolute CBF. [32] In addition, the ischemic thresholds for LDF have not been precisely defined for either global or focal cerebral ischemia. [33] Nevertheless, LDF accurately reflects relative changes in CBF, [32] and the magnitude of changes in CBF observed in our study are capable of producing cerebral infarction in other rat models of ischemia. [23,34]

Cerebral Ischemia After SAH

What are the likely explanations for the decreased cortical blood flow immediately after SAH that was observed in our model? Decreased CPP is one obvious factor: it occurred in all rats, was closely associated with the onset of decreased LDF, and the rates of change in CPP and LDF were similar while CPP was decreasing. However, LDF continued to fall while CPP rose toward baseline and reached its nadir more than 2 minutes after CPP did. In addition, no correlation was found between peak reductions in CPP and LDF. Finally, CPP returned to more than 70 mm Hg between 25 and 50 minutes after SAH, a level that does not normally reduce CBF, [35] while LDF remained approximately 50% below baseline. Thus, factors other than CPP are important contributors to acutely decreased cortical blood flow after SAH. Two other potential mechanisms are primary SAH-induced vasoconstriction and flow-metabolic coupling with a primary reduction in metabolic activity. Metabolic activity, as reflected by the EEG, decreased after SAH in all rats, but reached its nadir more than 1 minute after LDF. Therefore, it is unlikely that reduced EEG activity was the main cause of secondary reductions in cortical blood flow in this model.

Because LDF measurements depend on refraction of light, it is possible that direct interference with the laser signal by subarachnoid blood, rather than vasoconstriction or decreased CPP, could decrease LDF recordings in our model. We do not believe this played a significant role because slight pressure of the probe on the dura prevents the accumulation of subarachnoid blood under the probe, and LDF values decreased profoundly even in rats with little or no blood in the dorsal convexity subarachnoid space.

Vasoconstriction is the primary event underlying delayed cerebral ischemia after SAH, and a wide range of substrates have been implicated in its etiology. Hemoglobin and oxyhemoglobin cause vasoconstriction after SAH. [36] Although various potential mechanisms have been identified, [37-39] impairment of endothelium-dependent relaxation plays an important role in the process. [37] Recent studies have focused on the potent vasodilator and endothelium-derived relaxing factor nitric oxide (NO) or an NO-related compound in the control of normal vasodilatory tone [37] by a cyclic cGMP-dependent mechanism. [40] After SAH, hemoglobin and oxyhemoglobin can cause vasoconstriction by binding to NO and limiting its activity, [34] by decreasing cGMP levels, [41] or by generating cyclooxygenase products. [42]

Because of clinical interest in delayed cerebral vasospasm, many studies have emphasized the delayed effects of hemoglobin and NO synthase inhibitors. However, in animal models these substances have also been shown to cause early vasoconstriction. [7,10,12] In fact, a direct vasoconstrictive action of subarachnoid blood has been suggested as the primary cause of ischemia after SAH. [10] Our data indicate that both decreased CPP and direct vasoconstriction contribute to acute cerebral ischemia after SAH. During the first minute after the

onset of SAH, reduced CPP predominates in reducing blood flow. Secondary reductions are caused by independent factors such as vasoconstriction.

The importance of secondary ischemia (ie, ischemia unrelated to perfusion pressure) in the acute phases after SAH is unknown. However, the acutely decreased CBF and persistent hypoperfusion for at least 1 hour after SAH in our experimental model suggest that secondary ischemia may contribute significantly to neurological mortality and morbidity. This observation lends further support to the use of agents that could alter acute vasoconstriction or neuronal ischemic damage immediately after SAH. For example, attenuation of acute ischemic neuronal injury may contribute to the beneficial effects of nimodipine [43,44] and the 21-aminosteroids in SAH. [45,46] Further studies are needed to address this issue.

Conclusion

A noncraniotomy model of SAH has several advantages over models that require craniotomy, vessel avulsion, or injection of blood. Real-time recordings of LDF provide dynamic information about the causes of ischemia after SAH. Decreased CPP cannot fully explain acute cerebral ischemia after SAH, and there is evidence to support direct vasoconstriction as one additional mechanism. Further studies of this model of SAH are required to determine the physiological correlates of premature mortality, the incidence and cause of ischemic histological changes, the evidence for delayed vasospasm, and the effect on outcome of treating acute vasoconstriction and ischemia.

Ackno led ments

This research was supported by the Department of Neurosurgery at The Mount Sinai School of Medicine. The authors thank Stephen Ordway for editorial assistance.

R R C S

1. Broderick JP, Brott TG, Duldner JE, Tomsick T, Leach A. Initial and recurrent bleeding are the major causes of death following subarachnoid hemorrhage. Stroke. 1994;25:1342-1347. [Context Link]

2. Stoltenburg-Didinger G, Schwarz K. Brain lesions secondary to subarachnoid hemorrhage due to ruptured aneurysms. In: Cervos-Navarro J, Ferst R, eds. Stroke and Microcirculation. New York, NY: Raven Press Publishers; 1987:471-480. [Context Link]

3. Fisher CM. Clinical syndromes in cerebral thrombosis, hypertensive hemorrhage, and ruptured saccular aneurysm. Clin Neurosurg. 1975;22:117-147. [Context Link]

4. Nornes H. The role of intracranial pressure in the arrest of hemorrhage in patients with ruptured intracranial aneurysm. J Neurosurg. 1973;9:226-234. [Context Link]

5. Nornes H. Cerebral arterial flow dynamics during aneurysm haemorrhage. Acta Neurochir (Wien). 1978;41:39-48. [Context Link]

6. Dorsch NW, Branston NM, Symon L. Intracranial pressure changes following primate subarachnoid hemorrhage. Neurol Res. 1989;11:201-204. [Context Link]

7. Kuyama H, Ladds A, Branston NM, Nitta M, Symon L. An experimental study of acute subarachnoid haemorrhage in baboons: changes in cerebral blood volume, blood flow, electrical activity and water content. J Neurol Neurosurg Psychiatry. 1984;4:354-364. [Context Link]

8. McCormick PW, McCormick J, Zabramski JM, Spetzler RF. Hemodynamics of subarachnoid hemorrhage arrest. J Neurosurg. 1994;80:710-715. [Context Link]

9. Jakubowski J, Bell BA, Symon L, Zawirski MB, Francis DM. A primate model of subarachnoid hemorrhage: change in regional cerebral blood flow, autoregulation carbon dioxide reactivity, and central conduction time. Stroke. 1982;13:601-611. [Context Link]

10. Jakowski A, Crockard A, Burnstack G, Russel R, Kristek F. The time course of intracranial pathophysiological changes following experimental subarachnoid hemorrhage in the rat. J Cereb Blood Flow Metab. 1990;10:835-839. [Context Link]

11. Brawley B, Strandness D, Kelly W. The biphasic response of cerebral vasospasm in experimental subarachnoid hemorrhage. J Neurosurg. 1968;28:1-8. [Context Link]

12. Delgado TJ, Brismar J, Svendgaard NA. Subarachnoid hemorrhage in the rat: angiography and fluorescence microscopy of the major cerebral arteries. Stroke. 1985;16:595-602. [Context Link]

13. Diringer MN, Kirsch JR, Hanley DF, Traystman RJ. Altered cerebrovascular CO sub 2 reactivity following subarachnoid hemorrhage in cats. J Neurosurg. 1993;8:915-921. [Context Link]

14. Hauerberg J, Juhler M, Rasmussen G. Cerebral blood flow autoregulation after experimental subarachnoid hemorrhage during hyperventilation in rats. J Neurosurg Anesthesiol. 1993;5:258-263. [Context Link]

15. Kader A, Krauss WE, Onesti ST, Elliott JP, Solomon RA. Chronic cerebral blood flow changes following experimental subarachnoid hemorrhage in rats. Stroke. 1990;21:577-581. ibrar oldin s [Context Link]

16. Lewis PJ, Weir BK, Nosko MG, Tanabe T, Grace MG. Intrathecal nimodipine therapy in a primate model of chronic cerebral vasospasm. Neurosurgery. 1988;22:492-500. [Context Link]

17. Steiner L, Lofgren J, Zwetnow NN. Characteristics and limits of tolerance in repeated subarachnoid hemorrhage in dogs. Acta Neurol Scand. 1975;52:241-267. [Context Link]

18. Bederson JB, Gaurino L, Germano IM. Failure of changes in cerebral perfusion pressure to account for ischemia caused by subarachnoid hemorrhage: a new experimental model. J Neurosci. 1994;20:224. Abstract. [Context Link]

19. Barth KN, Onesti ST, Krauss WE, Solomon RA. A simple and reliable technique to monitor intracranial pressure in the rat: technical note. Neurosurgery. 1992;30:138-140. ibrar oldin s [Context Link]

20. Zea-Longa E, Weinstein PR, Carlson S, Cummins R. Reversible middle cerebral artery occlusion without craniectomy in rats. Stroke. 1992;20:84-91. [Context Link]

21. Bederson JB, Pitts LH, Tsuji M, Nishimura MC, Davis RL, Bartkowski H. Rat middle cerebral artery occlusion: evaluation of the model and development of a neurologic examination. Stroke. 1986;17:472-476. ibrar oldin s [Context Link]

22. Zar JH. Biostatistical Analysis. Englewood Cliffs, NJ: Prentice Hall; 1984:292-305. [Context Link]

23. Kaplan B, Brint S, Tanabe J, Jacewicz M, Wang X-J, Pulsinelli W. Temporal thresholds for neocortical infarction in rats subjected to reversible focal cerebral ischemia. Stroke. 1991;22:1032-1039. ibrar oldin s [Context Link]

24. Heiss WD, Podreka I. Role of PET and SPECT in the assessment of ischemic cerebrovascular disease. Cerebrovasc Brain Metab Rev. 1993;5:235-263. [Context Link]

25. Lewis DH, Eskridge JM, Newell DW, Grady MS, Cohen WA, Dalley RW, Loyd D, Grothaus-King A, Young P, Winn HR. Brain SPECT and the effect of cerebral angioplasty in delayed ischemia due to vasospasm. J Nucl Med. 1992;33:1789-1796. [Context Link]

26. Pupi A, De-Cristofaro MT, Passeri A, Castagnoli A, Santoro GM, Antoniucci D, Dal-Pozzo G, Pellicano G, Bacciottini L, Bottoncetti A. Quantitation of brain perfusion with 99mTc bicisate and single SPECT scan: comparison with microsphere measurements. J Cereb Blood Flow Metab. 1994;14:S28-S35. [Context Link]

27. Meixensberger J. Xenon 133-CBF measurements in severe head injury and subarachnoid haemorrhage. Acta Neurochir Suppl (Wien). 1993;9:28-33. [Context Link]

28. Rasmussen G, Hauerberg J, Waldemar G, Gjerris F, Juhler M. Cerebral blood flow autoregulation in experimental subarachnoid haemorrhage in rat. Acta Neurochir (Wien). 1992;119:128-133. [Context Link]

29. Nelson RJ, Perry S, Burns AC, Roberts J, Pickard JD. The effects of hyponatraemia and subarachnoid haemorrhage on the cerebral vasomotor responses of the rabbit. J Cereb Blood Flow Metab. 1991;11:661-666. [Context Link]

30. Takeuchi H, Handa Y, Kobayashi H, Kawano H, Hayashi M. Impairment of cerebral autoregulation during the development of chronic cerebral vasospasm after subarachnoid hemorrhage in primates. Neurosurgery. 1991;28:41-48. [Context Link]

31. Carpenter DA, Grubb RL Jr, Tempel LW, Powers WJ. Cerebral oxygen metabolism after aneurysmal subarachnoid hemorrhage. J Cereb Blood Flow Metab. 1991;11:837-844. [Context Link]

32. Dirnagl U, Kaplan B, Jacewicz M, Pulsinelli W. Continuous measurement of cerebral cortical blood flow by laser-Doppler flowmetry in a rat stroke model. J Cereb Blood Flow Metab. 1989;9:589-596. [Context Link]

33. Werner C. Laser Doppler flowmetry: a valid clinical tool? J Neurosurg Anesthesiol. 1993;5:139-141. [Context Link]

34. Nagasawa H, Kogure K. Correlation between cerebral blood flow and histologic changes in a new rat model of middle cerebral artery occlusion. Stroke. 1989;20:1037-1043. ibrar oldin s [Context Link]

35. Wagner EM, Traytsman R. Hydrostatic determinants of cerebral perfusion. Crit Care Med. 1986;114:484-490. [Context Link]

36. Macdonald RL, Weir BK. A review of hemoglobin and the pathogenesis of cerebral vasospasm. Stroke. 1991;22:971-982. ibrar oldin s [Context Link]

37. Faraci FM. Endothelium-derived vasoactive factors and regulation of the cerebral circulation. Neurosurgery. 1993;33:648-658. ibrar oldin s [Context Link]

38. Fuwa I, Mayberg M, Gadjusek C, Harada T, Luo Z. Enhanced secretion of endothelin by endothelial cells in response to hemoglobin. Neurol Med Chir (Tokyo). 1993;33:739-743. ibrar oldin s [Context Link]

39. Macrae IM, Robinson MJ, Graham DI, Reid JL, McCulloch J. Endothelin-l-induced reductions in cerebral blood flow: dose dependency, time course, and neuropathological consequences. Cereb Blood Flow Metab. 1993;13:276-284. [Context Link]

40. Moncada S, Palmer RMJ, Higgs EA. Nitric oxide: physiology, pathophysiology, and pharmacology. Pharmacol Rev. 1992;43:109-142. [Context Link]

41. Edwards DH, Byrne JV, Griffith TM. The effect of chronic subarachnoid hemorrhage on basal endothelium-derived relaxing factor activity in intrathecal cerebral arteries. J Neurosurg. 1992;76:830-837. [Context Link]

42. Toda N, Ayajiki K, Okarriura T. Endothelial modulation of contractions caused by oxyhemoglobin and N sup G-nitro-L-arginine in isolated dog and monkey cerebral arteries. Stroke. 1993;24:1584-1588. ibrar oldin s [Context Link]

43. Allen GS, Ahn HS, Preziosi TJ, Battye R, Boone SC, Chou SN, Kelly DL, Weir BK, Crabbe RA, Lavik PJ, Rosenbloom SB, Dorsey FC, Ingram CR, Mellits DE, Bertsch LA, Boisvert DP, Hundley MB, Johnson RK, Strom JA, Transou CR. Cerebral arterial spasm: a controlled trial of nimodipine in patients with subarachnoid hemorrhage. N Engl J Med. 1983;308:619-624. [Context Link]

44. Tettenborn D, Fierus M. Clinical aspects of nimodipine treatment in brain ischemia. Drugs Dev. 1993;2:473-482. [Context Link]

45. Kassell N, Haley EC, Alves W, Hansen CA. Phase III trial of tirilizad in aneurysmal subarachnoid hemorrhage. J Neurosci. 1994;80:383A. Abstract. [Context Link]

46. Hall ED, Travis MA. Effects of the nonglucocorticoid 21-aminosteroid U74006F on acute cerebral hypoperfusion following experimental subarachnoid hemorrhage. Exp Neurol. 1988;102:244-248. [Context Link]

IMA **A** **R**

Select All

Export Selected to PowerPoint

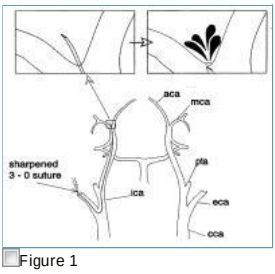

Figure 1

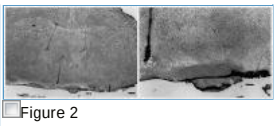

Figure 2

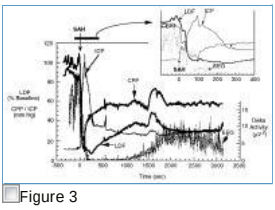

Figure 3

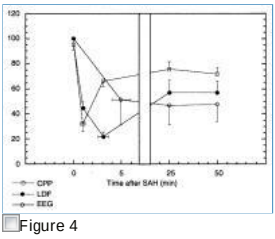

Figure 4

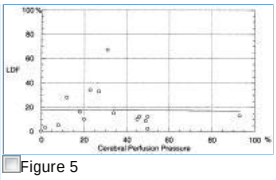

Figure 5

ack to **o**